Hepatitis C virus (HCV) protein expression enhances hepatic fibrosis in HCV transgenic mice exposed to a fibrogenic agent.

Philippe Chouteau, Nicole Defer, Alexandre Florimond, Julien Caldéraro, Martin Higgs, Aurore Gaudin, Emilie Mérour, Daniel Dhumeaux, Hervé Lerat, Jean-Michel Pawlotsky

Hepatitis C Virus (HCV) Protein Expression Enhances Hepatic Fibrosis in HCV Transgenic Mice Exposed to a Fibrogenic Agent

Philippe Chouteau,[1,2] Nicole Defer,[1] Alexandre Florimond,[1,2] Julien Caldéraro,[2,3] Martin Higgs,[1‡] Aurore Gaudin,[1] Emilie Mérour,[1] Daniel Dhumeaux,[1,2] Hervé Lerat,[1,2] and Jean-Michel Pawlotsky[1,2,4]

[1]Inserm U955, Créteil, France ; [2]Université Paris-Est, Créteil, France; [3]Department of Pathology, Hôpital Henri Mondor, Créteil, France, [4]National Reference Center for Viral Hepatitis B, C, and Delta, Department of Virology, Hôpital Henri Mondor, Créteil, France

[‡]Present address : Cancer Research UK Institute for Cancer Sciences, University of Birmingham, Birmingham, B15 2TT, UK

Corresponding Author: Prof. , MD, PhD, Department of Virology, Hôpital Henri Mondor, 51 avenue du Maréchal de Lattre de Tassigny, 94010 Créteil, France.

Tel : +33-1-4981-2827 ; Fax : +33-1-4981-4831

E-mail : jean-michel.pawlotsky@hmn.aphp.fr

Electronic word count: 5946

Abstract electronic word count: 244

Number of figures: 6

Number of tables: 1

List of abbreviations: HCV, hepatitis C virus; ORF, open reading frame; ECM, extra-cellular matrix; CCl_4, carbon tetrachloride; wt, wild-type; qPCR, quantitative PCR; hepatic stellate cells; HPCs, hepatic progenitor cells; PBS, phosphate buffer saline; CYP2E1, cytochrome P450 2E1; ROS, reactive oxygen species; BrdU, bromodeoxyuridine; ALT, alanine aminotransferase; AST, aspartate aminotransferase; CCL5, chemokine (C-C motif) ligand 5.

Conflict of interest: The authors declare that they have nothing to disclose regarding conflict of interest with respect to this manuscript.

Financial Support: This study was supported by the National Agency for Research on AIDS and Viral Hepatitis (ANRS; R0711JJ and R09017JJ). A. F. is the recipient of a postdoctoral fellowship from the French Ministry of Research; M. H. was the recipient of a postdoctoral fellowship from the ANRS.

ABSTRACT

Background & Aims: During chronic HCV infection, activation of fibrogenesis appears to be principally related to local inflammation. However, the direct role of hepatic HCV protein expression in fibrogenesis remains unknown.

Methods: We used transgenic mice expressing the full-length HCV open reading frame exposed to a 'second hit' of the fibrogenic agent carbon tetrachloride (CCl_4). Both acute and chronic liver injuries were induced in these mice by CCl_4 injections. Liver injury, expression of matrix re-modeling genes, reactive oxygen species (ROS), inflammation, hepatocyte proliferation, ductular reaction and hepatic progenitor cells (HPC) expansion were examined.

Results: After CCl_4 treatment, HCV transgenic mice exhibited enhanced liver fibrosis, significant changes in matrix re-modeling genes and increased ROS production compared to wt littermates despite no differences in the degree of local inflammation. This increase was accompanied by a decrease in hepatocyte proliferation, which appeared to be due to delayed hepatocyte entry into the S-phase. A prominent ductular reaction and hepatic progenitor cell compartment expansion were observed in transgenic animals. These observations closely mirror those previously made in HCV-infected individuals.

***Conclusions*:** Together, these results demonstrate that expression of the HCV proteins in hepatocytes contributes to the development of hepatic fibrosis in the presence of other fibrogenic agents. In the presence of CCl_4, HCV transgenic mice display an intra-hepatic re-organization of several key cellular actors in the fibrogenic process.

Keywords: hepatitis C virus; fibrosis; hepatocyte proliferation; reactive oxygen species; ductular reaction; hepatic progenitor cells

INTRODUCTION

Hepatic fibrosis, a result of active fibrogenesis, is a frequent feature of chronic hepatitis C virus (HCV) infection. Fibrogenesis is classically thought to be triggered principally by the local immune response. The role of HCV infection in fibrogenesis, in particular HCV protein expression in the liver, is unknown. Mice of the FL-N/35 lineage express the entire open reading frame (ORF) of a genotype 1b isolate of HCV in a liver-specific fashion [1]. In this model, the HCV proteins are expressed within hepatocytes at levels close to those observed in human infection, without infectious virus production or an antiviral immune response. These mice develop lesions similar to those observed during natural infection, including hepatic steatosis and hepatocellular carcinoma [2-6]. Preliminary observations suggested that FL-N/35 mice may be of interest in the study of liver fibrosis [1]. However, this model lacks the concomitant fibrogenesis triggers (such as liver inflammation) observed in HCV-infected individuals. Therefore, the effect of HCV protein expression on hepatic fibrosis in this model must be studied in the context of a 'second hit' of chronic liver injury.

The conventional paradigm of fibrogenesis in the liver is largely based on activation of fibrogenic processes associated with transformation of hepatic stellate cells (HSCs) into myofibroblast-like cells [7-10]. However, it remains paradoxical that, whereas HCV infection is present largely within hepatic lobules [11], fibrosis predominates in portal areas in chronically infected patients. Currently, there are no explanations for this observation, and the surrounding mechanisms remain

uninvestigated. One possible explanation is that viral particles produced within intralobular hepatocytes might directly activate periportal HSCs. Another non-exclusive explanation is that HCV infection may be accompanied by ductular proliferation [12].

In the normal liver, the replacement of necrotic and apoptotic hepatocytes occurs through replication of adjacent hepatocytes within the lobules. However, this primary pathway is impaired by a variety of insults, including viral infections [13, 14]. These situations have been shown to lead to proliferation of hepatic progenitor cells (HPCs) [15-17]. Such cells reside primarily in the periportal region and become the source of regenerating hepatocytes, as well as cholangiocytes and draining ductules [15, 18]. A by-product of the activation of this secondary proliferative pathway is a ductular reaction [15], which has been linked to fibrogenesis [19-28].

A strong correlation has been reported between HCV-related portal fibrosis and a periportal ductular reaction, with a relationship between the number of proliferating HPCs and the number of hepatocytes in replication arrest [29]. These observations support the hypothesis that portal fibrosis during chronic HCV infection may result from a periportal ductular reaction, possibly as a consequence of altered hepatocyte proliferation.

We illustrate below, using the FL-N/35 HCV transgenic mouse model in conjunction with an exogenous chemical fibrogenic agent, that the expression of HCV proteins *in vivo* plays a contributory role in the fibrogenic process, and is accompanied by a ductular reaction and a replicative arrest of intra-lobular hepatocytes concomitant with enhanced reactive oxygen species (ROS) production, in the absence of enhanced inflammation.

MATERIALS AND METHODS

Chemicals and antibodies

Carbon tetrachloride (CCl_4) and olive oil were purchased from Sigma-Aldrich (St. Louis, MO). Primary antibodies are described in more details in Supplementary Materials and Methods.

Animals

Wild-type mice (wt) and those transgenic for the entire HCV ORF (FL-N/35 lineage) were from the same genetic background (C57/Bl6) [1]. They were used in conformation with the European Community Council directive. Animals were bred and housed as previously described [2]. Studies were performed on age-matched 7- to 10-month old males.

<u>Chronic</u> CCl_4 treatment

Animals were injected intraperitoneally twice a week for 4 weeks with CCl_4 (0.5 μg/g of body weight) diluted in 5% olive oil, obtained the day of injection. Control mice were injected with an equal volume of olive oil. Twenty-four hours after the final injection, animals were sacrificed by CO_2 inhalation, and body and liver weights were measured. Sera (100 μL/mouse) and livers were immediately processed for enzymatic

assays and histological determination, or kept at -80 °C until processing.

Experimental acute liver injury and measurement of hepatocyte DNA synthesis

Mice were treated with a single intraperitoneal injection of CCl_4 (795 mg/kg body weight diluted in 5% olive oil). They were sacrificed at different time points after the injection. Bromodeoxyuridine (BrdU) was injected intraperitoneally (150 mg/kg of body weight) two hours prior to sacrifice. Hepatocyte DNA synthesis was measured by means of immunodetection of BrdU incorporation as described in Supplementary Materials and Methods.

Western blotting

Frozen liver tissues were processed as previously described [6]. The detailed procedure is described in Supplementary Materials and Methods.

Serum alanine aminotransferase and aspartate aminotransferase level measurements

Levels of alanine aminotransferase (ALT) and aspartate aminotransferase (AST) in the serum of mice were measured on a Cobas®6000 analyzer (Roche, Diagnostics, Basel, Switzerland), according to the manufacturer's instructions.

Liver histology and immunohistochemistry

Fresh liver tissues were fixed in 10% buffered formalin, paraffin-embedded, and 5 μm sections were prepared. Standard histology and immunostainings are described in Supplementary Materials and Methods.

Quantification of hepatocyte reactive oxygen species (ROS)

Frozen liver sections (10 μm) from wt and FL-N/35 mice were assessed for the presence of ROS, as previously described [4]. The percentage of ROS-specific hepatocytes was calculated, and normalized to that in wt controls. In all cases (CCl_4-treated and untreated mice), only large cells with round nuclei present within the parenchyma were considered as hepatocytes.

RNA isolation and quantitative real-time PCR analysis

Total RNA and complementary DNA were purified and synthesized, respectively, as previously described [6]. Quantitative PCR was performed with an Applied Biosystems 7300 Thermal Cycler using Taqman reagents (Applied Biosystems), as described in Supplementary Materials and Methods.

Measurement of CCL5 protein in liver tissues

CCL5 protein was quantified in frozen liver tissues according to the procedure described in Supplementary Materials and Methods.

Image analysis

Tissue sections were photographed using a Zeiss Axioskop 40 microscope in conjunction with a Zeiss MRc5 Axiocam and Axiovision LE software (Zeiss, Jena, Germany). Image analyses were performed as described in Supplementary Materials and Methods.

Statistical analyses

Statistical analyses were performed using Prism software (GraphPad Software Inc., La Jolla, CA). Results are expressed as mean±standard error of the mean (SEM). Box-and-whisker graphs are used; the line in the middle is the median, the box extends from the 25th to the 75th percentile, and the whiskers extend to the lowest and highest values. To determine the statistical significance of the data, Mann-Whitney non-parametrical tests were performed. Pearson's correlation coefficient was used to determine correlations between continuous normally distributed variables. All *P* values were two-tailed, with *P* values less than 0.05 considered as significant.

RESULTS

Hepatic expression of the full-length HCV ORF enhances liver fibrosis induced by CCl_4 in HCV transgenic mice

The extent of extracellular matrix (ECM) deposition occurring within the liver of wt and FL-N/35 mice chronically exposed to CCl_4 was determined by picrosirius red staining of formalin-fixed, paraffin-embedded liver sections. As shown in Fig. 1A and 1B, ECM deposition was observed only in normal anatomical structures such as portal tracts in untreated FL-N/35 and wt mice. Thus, in the absence of an exogenous fibrogenic stimulus, expression of the HCV proteins does not *per se* stimulate ECM deposition at a level detectable using picrosirius staining.

In CCl_4-treated wt and FL-N/35 animals, picrosirius red staining demonstrated established fibrosis with distinctive septa-like morphologies (Fig. 1A and 1B). In both transgenic and nontransgenic animals, the quantity of ECM was significantly greater than in the corresponding untreated animals (Fig. 1B). In CCl_4-treated mice, the quantity of ECM was significantly greater in FL-N/35 than in wt animals (median collagen deposition: 1.7, range 1.0-2.8 *vs* 1.2, range, 0.9-2.4; P=0.0039) (Fig. 1B).

As differences in the expression of cytochrome P450 2E1 (CYP2E1), the enzyme responsible for bioactivation of CCl_4, could be responsible for the observed difference [30], we quantified CYP2E1 expression by western blotting in HCV transgenic and wt animals. No difference was found between the two groups (Supplementary Fig. S1).

Overall, these results suggest that intrahepatic expression of the HCV proteins *in vivo* potentiates the fibrogenic effect of the exogenous agent CCl_4.

Increased liver fibrosis induced by CCl_4 in transgenic mice is not due to a higher degree of necroinflammation in the presence of HCV proteins

We examined the role of HCV protein expression in liver necroinflammation in the presence and absence of CCl_4. Hematoxylin-eosin staining of liver tissues showed normal hepatic architecture in wt and FL-N/35 mice that did not receive CCl_4 (Supplementary Fig. S2). In contrast, CCl_4-treated animals showed remnants of degenerated and ballooned/necrotic hepatocytes, equivalently present in wt and FL-N/35 mice. Mild mononuclear cell infiltration in the same areas was also evenly present in these animals.

Expression of F4/80 mRNA, a marker of resident and recruited macrophages, did not differ between untreated wt and FL-N/35 animals. F4/80 mRNA expression was induced to the same degree in both transgenic and non-transgenic mice after chronic CCl_4 administration (Supplementary Fig. S3). Immunostaining of liver tissues with the pan-T lymphocyte marker CD3 revealed similar degrees of T lymphocyte infiltration in wt and FL-N/35 mice exposed to CCl_4, with CD3-positive cells present along hepatic septa (Supplementary Fig. S4).

The chemokine CCL5 is secreted by T-cells and macrophages and could play a role in fibrosis by stimulating hepatic stellate cells [31]. CCL5 expression did not differ between wt and FL-N/35 animals, both in the presence and absence of CCl_4 (Supplementary Figs. S5 and S6).

Taken together, these results suggest that enhanced fibrosis in HCV-transgenic mice exposed to CCl_4 is not mediated by an increased necroinflammation.

Increased liver fibrosis induced by CCl_4 in transgenic mice is associated with alterations in the expression of genes involved in ECM remodeling

We measured the hepatic expression of a number of ECM remodeling genes, including genes coding for ECM components (collagens), proteins involved in ECM production/degradation (matrix metalloproteinases [MMP]) and regulators of MMPs (tissue inhibitors of metalloproteinase [TIMP]) in the different groups of mice. As shown in Fig. 2, in the absence of an exogenous fibrogenic stimulus, the expression of HCV proteins in hepatocytes was not associated with higher levels of expression of these genes. In CCl_4-treated wt animals, expression of all of the tested mRNA levels was significantly modified compared to the untreated mice, but in various directions (Fig. 2). Among the different collagen genes tested, only collagen 1α1 expression was notably enhanced in FL-N/35 compared to wt CCl_4-treated mice, although the results did not reach statistical significance (p = 0,055). The expression of the other collagens showed no difference (Fig. 2A). MMP7 mRNA levels were significantly lower in HCV transgenic than in non-transgenic CCl_4-treated animals, whereas the expression of MMP13, MMP3 and TIMP1 was notably but not significantly lower (p values between 0.052 and 0.055, Fig. 2B and 2C). These results were in keeping with the increase in ECM deposition observed in HCV transgenic animals treated with CCl_4.

Liver fibrosis is associated with decreased hepatocyte proliferation in HCV transgenic mice chronically exposed to CCl_4

Since hepatic fibrosis in HCV-infected patients has been associated with increased hepatocyte replicative arrest [29], we next examined the extent of hepatocyte proliferation in wt and FL-N/35 mice in the presence and absence of CCl_4. Hepatocyte proliferation was evaluated by immunohistochemistry for Ki67, a nuclear antigen that is expressed in G1, S, G2 and M phases of the cell cycle, but absent in G0 or quiescent phase. In the absence of chronic CCl_4 exposure, a very low proportion of proliferative hepatocytes was observed in both wt and FL-N/35 mice, with no differences between these two groups, suggesting low-level basal renewal of the mature hepatocyte pool in the parenchyma (Fig. 3A and 3B).

As a consequence of chronic exposure to CCl_4, hepatocyte proliferation was significantly increased in both wt and FL-N/35 mice compared to non-exposed animals (Fig. 3A and 3B). As shown in Fig. 3B, hepatocyte proliferation was significantly lower in CCl_4-exposed FL-N/35 than in wt mice (median positive hepatocytes, 25.1 %, range 7.1-65.7 %, *vs* 30.3 %, range 5.9-49.2 %, respectively; P=0.002). No difference in the distribution of proliferating hepatocytes within the parenchyma was observed between treated wt and FL-N/35 animals.

In HCV-transgenic mice exposed to CCl_4, a significant inverse relationship between the number of Ki67 positive hepatocytes and the extent of ECM deposition was observed (r=0.893, P=0.012; Fig. 3C). In contrast, no correlation was found in CCl_4-exposed wt mice (r=0.1022, P=0.81; Fig. 3D).

In concert, these results suggest that fibrosis induced by CCl_4 exposure in the context of HCV protein expression is concomitant with a lowered capability of hepatocytes to regenerate.

A prominent ductular reaction is present in HCV transgenic mice chronically exposed to CCl_4

Since decreased hepatocyte proliferation has been linked with the development of a ductular reaction in several hepatic disorders, in particular in HCV infection [29, 32], we next studied the ductular reaction in both wt and FL-N/35 mice by immunochemistry for cytokeratin 19 (CK19), a common bile duct, ductular epithelium and HPC marker in murine tissues. CK19-positive staining was limited to bile duct cholangiocytes in untreated wt and FL-N/35 mice, with no differences between the two groups (Fig. 4A and 4B).

Exposure of wt animals to CCl_4 did not modify the quantity and distribution of CK19-positive biliary epithelium (Fig. 4A and 4B). In contrast, HCV transgenic animals chronically exposed to CCl_4 presented a prominent positive staining for CK19, distributed at the periphery of the portal areas, in chords, clumps and rings, quite distinct from the anatomical bile ducts (Fig. 4A). The area occupied by CK19-positive biliary epithelium, comprising both anatomical bile ducts and the ductular reaction, was increased nearly 3-fold compared with CCl_4-exposed wt mice (0.59% and 0.18% respectively, P=0.0016; Fig. 4B).

Altogether, these results suggest that fibrosis induced by CCl_4 exposure in the context of HCV protein expression is concomitant with a ductular reaction, which is absent in similarly treated wt animals.

The ductular reaction is associated with expansion of the HPC population in HCV transgenic mice chronically exposed to CCl_4

Since hepatic fibrosis in HCV-infected patients has been associated with increased HPC expansion [29], we assessed whether the increased ductular reaction was associated with expansion of the HPC population in HCV transgenic animals exposed to CCl_4. HPCs were distinguished from cholangiocytes as being CK19-positive cells distal to sites of ductular reaction and isolated within the parenchyma, without the cord-like arrangement of the ductules. In the absence of CCl_4, a few HPCs were visible in the livers from either wt or FL-N/35 mice (Fig. 4A and 4C). After chronic CCl_4 treatment, a non-significant trend towards a higher number of isolated CK19-positive cells than in the untreated animals was observed in wt mice (Fig. 4A and 4C). In CCl_4-treated FL-N/35 mice, a statistically significant increase in CK19-positive cells was observed when compared to CCl_4-treated wt mice (P=0.0016; Fig. 4C).

We observed significant correlations between the number of HPCs per portal tract and the extent of ECM deposition (r=0.71, P=0.0062; Fig. 4D), and between the number of HPCs and the surface of the ductular reaction (r=0.7984, P=0.0011; Fig. 4E), which were independent of HCV protein expression. However, FL-N/35 animals displayed increased ECM deposition, an increased number of HPCs per portal tract, and a larger ductular reaction when compared with wt animals, suggesting that the viral proteins may exacerbate these phenomena.

Together, these data indicate that the increased ductular reaction observed in HCV transgenic mice is associated with expansion of the HPC population.

The expansion of the HPC population leads to normal liver reconstitution in HCV transgenic mice chronically exposed to CCl_4

As shown in Table 1, despite the decreased hepatocyte proliferation in FL-N/35 transgenic mice chronically exposed to CCl_4 shown in Figs. 3A and 3B, no difference was observed in body or liver weights between olive oil- and CCl_4-treated animals in both wt and FL-N/35 groups, suggesting that liver tissue reconstitution is not substantially impaired in HCV transgenic mice.

Hepatocyte cell cycle progression is impaired after acute liver injury in HCV transgenic mice

In order to assess whether HCV protein expression impairs liver regeneration, hepatocyte proliferation was measured in both wt and FL-N/35 mice during the course of acute CCl_4-induced liver injury (Fig. 5A). Analysis of BrdU incorporation showed no or very few BrdU-positive cells in wt and HCV transgenic mouse livers before CCl_4 injection (0h), indicating that the majority of liver cells were quiescent in G0. As shown in Fig. 5A and 5B, both wt and HCV transgenic animals showed a significant increase of BrdU-positive hepatocytes after CCl_4 injection, suggesting entry into the S-phase of the cell cycle. However, this phenomenon was delayed in HCV transgenic animals, with a peak of BrdU incorporation reached at 48 hours post-injection, compared to 40 hours post-injection in wt animals (Fig. 5B). These findings indicate that HCV protein expression is associated with a delay in early cell cycle progression after acute liver injury.

ROS production is enhanced in HCV transgenic mice treated or not with CCl_4

Since oxidative stress has been reported to modulate the fibrogenic response and elevated ROS production is frequently observed in HCV infected cells [33, 34], we measured ROS levels in the livers of wt and FL-N/35 mice. Using dihydroethidium (DHE) as a marker for intracellular ROS, we found that hepatocyte-specific ROS levels were significantly higher in frozen liver sections from HCV transgenic mice compared to their wt littermates in the absence of CCl_4 treatment (Fig. 6A, upper panels and Fig. 6B), In CCl_4-treated animals, ROS levels were significantly higher than in untreated animals in both the wt and FL-N/35 groups (Fig. 6A, lower panels), principally due to infiltrating cells. However, when ROS production was measured only in hepatocytes, the levels were significantly higher in CCl_4-exposed FL-N/35 mice than in their wt counterpart animals (Fig. 6A, lower panels and Fig. 6B). These results show that intrahepatic expression of the HCV proteins is associated with enhanced baseline ROS levels and that this phenomenon is amplified by CCl_4 treatment.

DISCUSSION

Several *in vitro* reports have suggested that HCV proteins can directly induce fibrogenetic processes. For example, it has been shown that the culture medium of Huh7 cells harboring the HCV subgenomic replicon is able to activate *in vitro*-cultured HSCs, demonstrating that virus production is not a pre-requisite for such activation [35]. Moreover, the core and nonstructural 5A (NS5A) proteins have been suggested to play

a direct role in the alteration of the hepatocyte metabolism, partly *via* mitochondrial deregulation which generates ROS, strong inducers of pro-fibrogenic cytokines within the liver [1, 36, 37].

The mouse model used in this study is ideal to assess the effect of HCV protein expression on a liver phenomenon. Indeed, these mice specifically express the different HCV proteins in the liver; however, they are unable to reproduce the complete HCV life cycle, because the transgene is composed of a cDNA corresponding to the full-length polyprotein coding region, whereas the 5' and 3' untranslated sequences of the viral genome necessary for replication of viral RNA are lacking [1].

Our findings suggest that HCV protein expression *per se* is not able to induce fibrosis at a level detectable by common histological and molecular techniques. Nevertheless, we demonstrate for the first time that hepatic expression of the full-length HCV ORF *in vivo* is able to enhance fibrosis induced by another fibrogenic agent, a context similar to chronic human infection where a number of fibrogenic triggers are present in the liver. Importantly, this effect is independent of the degree of local inflammation. Our finding that ROS production is significantly increased in HCV transgenic hepatocytes, both in the absence and presence of CCl_4 treatment, could at least partly explain that HCV transgenic mice are more susceptible to the development of liver fibrosis when they are exposed to a 'second hit' by a fibrogenic agent.

We show that enhanced liver fibrosis in HCV transgenic animals is associated with a deregulation of the expression of several matrix remodeling genes. This includes down-regulation of the expression of MMP13, a protease that specifically degrades collagen 1, TIMP1, a protein that inhibits MMPs active forms [38], and MMP3, an activator of pro-MMPs. Thus, HCV transgenic animals seem to be less able to degrade

collagen 1, thereby favoring ECM deposition. In addition, the expression of MMP7, a protease implicated in nerve growth factor-dependent myofibroblast survival [39], was reduced in CCl_4-treated HCV mice, whereas a similar trend was found in untreated transgenic animals, suggesting that HCV protein expression could protect hepatic myofibroblasts from apoptosis, thus prolonging fibrosis signals.

In our study, the enhancement of fibrosis induced by another fibrogenic agent in transgenic mice expressing the full-length HCV ORF is accompanied by reduced hepatocyte proliferation, which correlates with the stage of fibrosis. The replacement of hepatocytes lost from normal hepatic parenchyma is known to occur through replication of mature hepatocytes [16]. Inhibition of hepatocyte replication by drugs [16], alcohol [40], steatosis [15] or viral infection [14, 29] promotes the activation of a secondary replicative pathway involving bipotential HPCs [16]. The activation of HPCs subsequently leads to the production of both hepatocytes and cholangiocytes, and the onset of a ductular reaction. The results presented here show that hepatocytes expressing the full HCV ORF exhibit defective replication after treatment with CCl_4. Our acute liver injury experiments suggest that this effect is, at least in part, due to a delayed entry of hepatocytes into the S-phase of the cell cycle.

The defective replication of HCV-expressing hepatocytes leads to the activation of the HPC pathway and subsequent amplification of the HPC population. In keeping with this hypothesis, we observed reduced proliferation of mature hepatocytes together with a marked increase in the number of activated HPCs and a prominent ductular reaction in CCl_4-treated FL-N/35 mice. A strong relationship between hepatic fibrosis severity and the intensity of the ductular reaction has been reported in both rodents and

humans [29, 32, 41, 42]. A similar relationship is shown here in the FL-N/35 mouse strain in the context of HCV protein-induced liver fibrosis [29].

In summary, we have shown that transgenic mice expressing the full-length HCV ORF develop more severe hepatic fibrosis after chronic CCl_4 exposure than nontransgenic animals. This effect is not linked to local inflammation alterations induced by HCV proteins. Like during chronic HCV infection in humans, enhanced fibrosis in HCV transgenic mice is associated with a pronounced ductular reaction, HPC activation and a concomitant reduction in hepatocyte proliferation that appears to be in part due to a delayed entry of hepatocytes into the S-phase of the cell cycle. In addition, HCV-related fibrosis is associated with deregulation of the expression of several matrix remodeling genes and enhanced ROS production that likely participate in the fibrogenic process. Overall, our findings in HCV transgenic mice show that expression of the HCV proteins in hepatocytes contributes to the development of hepatic fibrosis in the presence of other fibrogenic agents, a situation close to human infection.

REFERENCES

[1] Lerat H, Honda M, Beard MR, Loesch K, Sun J, Yang Y, et al. Steatosis and liver cancer in transgenic mice expressing the structural and nonstructural proteins of hepatitis C virus. Gastroenterology 2002;122:352-365.

[2] Disson O, Haouzi D, Desagher S, Loesch K, Hahne M, Kremer EJ, et al. Impaired clearance of virus-infected hepatocytes in transgenic mice expressing the hepatitis C virus polyprotein. Gastroenterology 2004;126:859-872.

[3] Lerat H, Kammoun HL, Hainault I, Merour E, Higgs MR, Callens C, et al. Hepatitis C virus proteins induce lipogenesis and defective triglyceride secretion in transgenic mice. J Biol Chem 2009;284:33466-33474.

[4] Nishina S, Hino K, Korenaga M, Vecchi C, Pietrangelo A, Mizukami Y, et al. Hepatitis C virus-induced reactive oxygen species raise hepatic iron level in mice by reducing hepcidin transcription. Gastroenterology 2008;134:226-238.

[5] Simonin Y, Disson O, Lerat H, Antoine E, Biname F, Rosenberg AR, et al. Calpain activation by hepatitis C virus proteins inhibits the extrinsic apoptotic signaling pathway. Hepatology 2009;50:1370-1379.

[6] Higgs MR, Lerat H, Pawlotsky JM. Downregulation of Gadd45beta expression by hepatitis C virus leads to defective cell cycle arrest. Cancer Res 2010;70:4901-4911.

[7] De Leeuw AM, McCarthy SP, Geerts A, Knook DL. Purified rat liver fat-storing cells in culture divide and contain collagen. Hepatology 1984;4:392-403.

[8] Friedman SL. Mechanisms of disease: Mechanisms of hepatic fibrosis and therapeutic implications. Nat Clin Pract Gastroenterol Hepatol 2004;1:98-105.

[9] Friedman SL, Roll FJ. Isolation and culture of hepatic lipocytes, Kupffer cells, and sinusoidal endothelial cells by density gradient centrifugation with Stractan. Anal Biochem 1987;161:207-218.

[10] Kent G, Gay S, Inouye T, Bahu R, Minick OT, Popper H. Vitamin A-containing lipocytes and formation of type III collagen in liver injury. Proc Natl Acad Sci USA 1976;73:3719-3722.

[11] Liang Y, Shilagard T, Xiao SY, Snyder N, Lau D, Cicalese L, et al. Visualizing hepatitis C virus infections in human liver by two-photon microscopy. Gastroenterology 2009;137:1448-1458.

[12] Roskams TA, Theise ND, Balabaud C, Bhagat G, Bhathal PS, Bioulac-Sage P, et al. Nomenclature of the finer branches of the biliary tree: canals, ductules, and ductular reactions in human livers. Hepatology 2004;39:1739-1745.

[13] Marshall A, Rushbrook S, Davies SE, Morris LS, Scott IS, Vowler SL, et al. Relation between hepatocyte G1 arrest, impaired hepatic regeneration, and fibrosis in chronic hepatitis C virus infection. Gastroenterology 2005;128:33-42.

[14] Wagayama H, Shiraki K, Yamanaka T, Sugimoto K, Ito T, Fujikawa K, et al. p21WAF1/CTP1 expression and hepatitis virus type. Dig Dis Sci 2001;46:2074-2079.

[15] Oben JA, Roskams T, Yang S, Lin H, Sinelli N, Li Z, et al. Sympathetic nervous system inhibition increases hepatic progenitors and reduces liver injury. Hepatology 2003;38:664-673.

[16] Bissell DM, Roulot D, George J. Transforming growth factor beta and the liver. Hepatology 2001;34:859-867.

[17] Yang S, Koteish A, Lin H, Huang J, Roskams T, Dawson V, et al. Oval cells compensate for damage and replicative senescence of mature hepatocytes in mice with fatty liver disease. Hepatology 2004;39:403-411.

[18] Roskams T, De Vos R, Van Eyken P, Myazaki H, Van Damme B, Desmet V. Hepatic OV-6 expression in human liver disease and rat experiments: evidence for hepatic progenitor cells in man. J Hepatol 1998;29:455-463.

[19] Glaser SS, Gaudio E, Miller T, Alvaro D, Alpini G. Cholangiocyte proliferation and liver fibrosis. Expert Rev Mol Med 2009;11:e7.

[20] Grappone C, Pinzani M, Parola M, Pellegrini G, Caligiuri A, DeFranco R, et al. Expression of platelet-derived growth factor in newly formed cholangiocytes during experimental biliary fibrosis in rats. J Hepatol 1999;31:100-109.

[21] Herbst H, Frey A, Heinrichs O, Milani S, Bechstein WO, Neuhaus P, et al. Heterogeneity of liver cells expressing procollagen types I and IV in vivo. Histochem Cell Biol 1997;107:399-409.

[22] Malizia G, Brunt EM, Peters MG, Rizzo A, Broekelmann TJ, McDonald JA. Growth factor and procollagen type I gene expression in human liver disease. Gastroenterology 1995;108:145-156.

[23] Milani S, Herbst H, Schuppan D, Surrenti C, Riecken EO, Stein H. Cellular localization of type I, III and IV procollagen gene transcripts in normal and fibrotic human liver. Am J Pathol 1990;137:59-70.

[24] Paradis V, Dargere D, Vidaud M, de Gouville A-C, Huet S, Martinez V, et al. Expression of connective tissue growth factor in experimental rat and human liver fibrosis. Hepatology 1999;30:968-976.

[25] Pinzani M, Milani S, De Franco R, Grappone C, Caligiuri A, Gentilini A, et al. Endothelin 1 is overexpressed in human cirrhotic liver and exerts multiple effects on activated hepatic stellate cells. Gastroenterology 1996;110:534-548.

[26] Ramm GA, Nair VG, Bridle KR, Shepherd RW, Crawford DHG. Contribution of hepatic parenchymal and nonparenchymal cells to hepatic fibrogenesis in biliary atresia. Am J Pathol 1998;153:527-535.

[27] Sedlaczek N, Jia J-D, Bauer M, Herbst H, Ruehl M, Hahn EG, et al. Proliferating bile duct epithelial cells are a major source of connective tissue growth factor in rat biliary fibrosis. Am J Pathol 2001;158:1239-1244.

[28] Wynn TA, Barron L. Macrophages: master regulators of inflammation and fibrosis. Semin Liver Dis 2010;30:245-257.

[29] Clouston AD, Powell EE, Walsh MJ, Richardson MM, Demetris AJ, Jonsson JR. Fibrosis correlates with a ductular reaction in hepatitis C: roles of impaired replication, progenitor cells and steatosis. Hepatology 2005;41:809-818.

[30] Weber LW, Boll M, Stampfl A. Hepatotoxicity and mechanism of action of haloalkanes: carbon tetrachloride as a toxicological model. Critical Rev Toxicol 2003;33:105-136.

[31] Berres ML, Koenen RR, Rueland A, Zaldivar MM, Heinrichs D, Sahin H, et al. Antagonism of the chemokine CCl5 ameliorates experimental liver fibrosis in mice. J Clin Invest 2010;120:4129-4140.

[32] Richardson MM, Jonsson JR, Powell EE, Brunt EM, Neuschwander-Tetri BA, Bhathal PS, et al. Progressive fibrosis in nonalcoholic steatohepatitis: association with altered regeneration and a ductular reaction. Gastroenterology 2007;133:80-90.

[33] Novo E, Parola M. Redox mechanisms in hepatic chronic wound healing and fibrogenesis. Fibrogenesis Tissue Repair 2008;1:5.

[34] Simula MP, De Re V. Hepatitis C virus-induced oxidative stress and mitochondrial dysfunction: a focus on recent advances in proteomics. Proteomics Clin Appl 2010;4:782-793.

[35] Schulze-Krebs A, Preimel D, Popov Y, Bartenschlager R, Lohmann V, Pinzani M, et al. Hepatitis C virus-replicating hepatocytes induce fibrogenic activation of hepatic stellate cells. Gastroenterology 2005;129:246-258.

[36] Gong G, Waris G, Tanveer R, Siddiqui A. Human hepatitis C virus NS5A protein alters intracellular calcium levels, induces oxidative stress, and activates STAT-3 and NF-kappa B. Proc Natl Acad Sci USA 2001;98:9599-9604.

[37] Moriya K, Nakagawa K, Santa T, Shintani Y, Fujie H, Miyoshi H, et al. Oxidative stress in the absence of inflammation in a mouse model for hepatitis C virus-associated hepatocarcinogenesis. Cancer Res 2001;61:4365-4370.

[38] Denhardt DT, Feng B, Edwards DR, Cocuzzi ET, Malyankar UM. Tissue inhibitor of metalloproteinases (TIMP, aka EPA): structure, control of expression and biological functions. Pharmacol Ther 1993;59:329-341.

[39] Kendall TJ, Hennedige S, Aucott RL, Hartland SN, Vernon MA, Benyon RC, et al. p75 neurotrophin receptor signaling regulates hepatic myofibroblast proliferation and apoptosis in recovery from rodent liver fibrosis. Hepatology 2009;49:901-910.

[40] Crary GS, Albrecht JH. Expression of cyclin-dependent kinase inhibitor p21 in human liver. Hepatology 1998;28:738-743.

[41] Lowes KN, Brennan BA, Yeoh GC, Olynyk JK. Oval cell numbers in human chronic liver diseases are directly related to disease severity. Am J Pathol 1999;154:537-541.

[42] Knight B, Akhurst B, Matthews VB, Ruddell RG, Ramm GA, Abraham LJ, et al. Attenuated liver progenitor (oval) cell and fibrogenic responses to the choline deficient, ethionine supplemented diet in the BALB/c inbred strain of mice. J Hepatol 2007;46:134-141.

FIGURE LEGENDS

Fig 1. Histological analysis of liver fibrosis in wt and FL-N/35 mice in the absence or presence of chronic CCl_4 exposure. (A) Representative images of picrosirius red-staining of liver sections from olive-oil and CCl_4-injected wt and FL-N/35 animals. Scale bars: 100 µm. **(B)** Quantification of picrosirius red-staining from images from various lobes of each liver (6 to 10 images per liver). NS: not significant.

Fig. 2. mRNA level quantification of genes involved in ECM remodeling in the livers of wt and FL-N/35 mice in the absence or presence of chronic CCl_4 exposure. mRNA levels of collagens **(A)**, MMPs **(B)** and TIMPs **(C)** were measured by means of qRT-PCR. mRNA levels were normalized to the expression of actin; values are expressed as the percentage of wt animals treated with olive oil (OO).

Fig. 3. Hepatocyte proliferation in wt and FL-N/35 mice in the absence or presence of chronic CCl_4 exposure. (A) Representative images of Ki67 immunostaining of liver sections from olive-oil and CCl_4-treated wt and FL-N/35 animals. Positive Ki67 nuclei are indicated with arrows. Scale bars: 100 µm. **(B)** Quantification of Ki67-positive hepatocytes from various lobes of each liver. Data are expressed as a percentage of total hepatocytes per field. NS: not significant. **(C)** Relationship between hepatocyte proliferation and the extent of CCl_4-induced ECM deposition in HCV-transgenic mice treated with CCl_4. Data points represent individual animals. Analysis was performed with 9 animals from 2 independent experiments. **(D)** Relationship between hepatocyte

proliferation and the extent of CCl_4-induced ECM deposition in wt mice treated with CCl_4. Data represents 8 animals from 2 independent experiments.

Fig. 4. Ductular reaction in the livers of wt and FL-N/35 mice in the absence or presence of chronic CCl_4 exposure. (A) CK19-immunostaining of liver sections from olive oil- and CCl_4-treated wt and FL-N/35 animals. Open arrows indicate CK19-positive bile ducts. Black arrows indicate prominent ductules. Arrowheads indicate hepatic progenitor cells (HPCs). The two lower images show higher magnifications. **(B)** Quantification of the ductular reaction (CK19-positive bile ducts) in images of CK19 immunostaining of olive oil- and CCl_4-treated animals. (C) Quantification of isolated HPCs (isolated CK19-positive cells nearby portal tracts) in images of CK19 immunostaining of olive oil- and CCl_4-treated animals. (D) Relationship between the number of HPCs and the extent of CCl_4-induced ECM deposition. (E) Relationship between the extent of the ductular reaction and the number of HPCs.

Fig. 5. Hepatocyte DNA synthesis in wt and FL-N/35 mice after acute liver injury caused by high-dose CCl_4 Injection. (A) Representative photomicrographs of BrdU immuno-histochemical staining in acutely injured livers from wt and FL-N/35 mice at 0h, 24h, 40h, 48h and 60h post CCl_4 injection. BrdU-positive nuclei are stained in red. Scale bars = 100 µm. **(B)** BrdU incorporation at 0h, 24h, 40h, 48h and 60h post CCl_4 injection in wt and FL-N/35 animals. The number of BrdU-positive hepatocytes was expressed per μm^2 of tissue area.

Fig. 6. Quantification of ROS levels in the livers of wt and FL-N/35 mice in the absence or presence of chronic CCl_4 exposure. (A) Frozen 10 µm liver sections of olive oil and CCl_4-treated wt and FL-N/35 mice were stained with DHE and DAPI (insert), and analyzed by fluorescence microscopy. Representative examples are shown. Scale bars = 50 µm. **(B)** The number of ROS-positive hepatocytes was measured, and is shown as the percentage of ROS-positive cells as described in the Material and Methods section.

Table 1. Age, body and liver weights and ALT/AST levels in wt and FL-N/35 mice chronically exposed or not to CCl_4. Mean±SEM values are shown. NS: not significant.

	Olive oil		p	CCl_4		p
	wt (n=15)	FL-N/35 (n=15)		wt (n=13)	FL-N/35 (n=17)	
Age (month)	8-10	8-10		8-10	8-10	
Body weight (g)	33.7±0.8	33.9±1.2	NS	30.0±3.5	31.3±3.9	NS
Liver weight (g)	1.5±0.04	1.5±0.09	NS	1.5±0.3	1.4±0.4	NS
ALT (IU/mL)	42±12.6	46±22.8	NS	2570.5±479.5	1654.8±316.9	NS
AST (IU/mL)	63.2±20.7	81.6±32.8	NS	1532.5±319.7	921±170	NS

Figure 1A

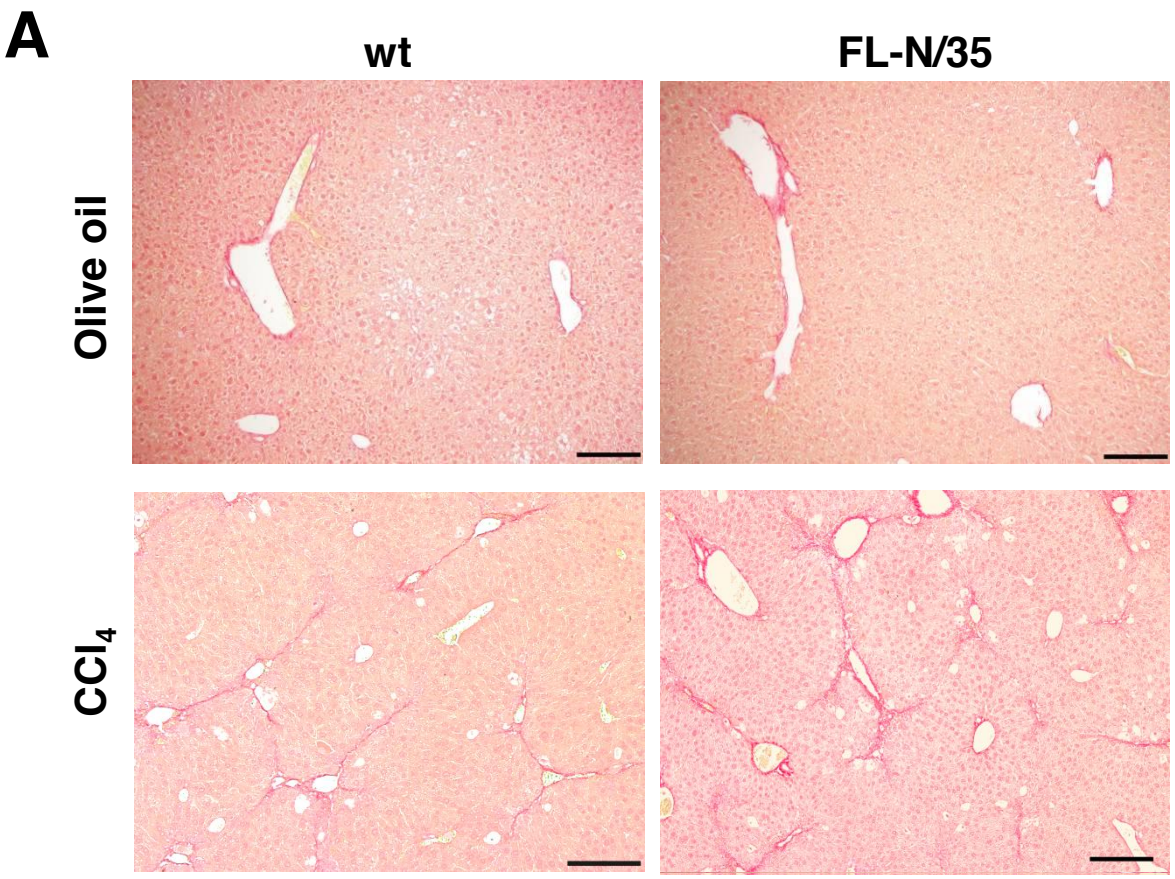

Figure 1B

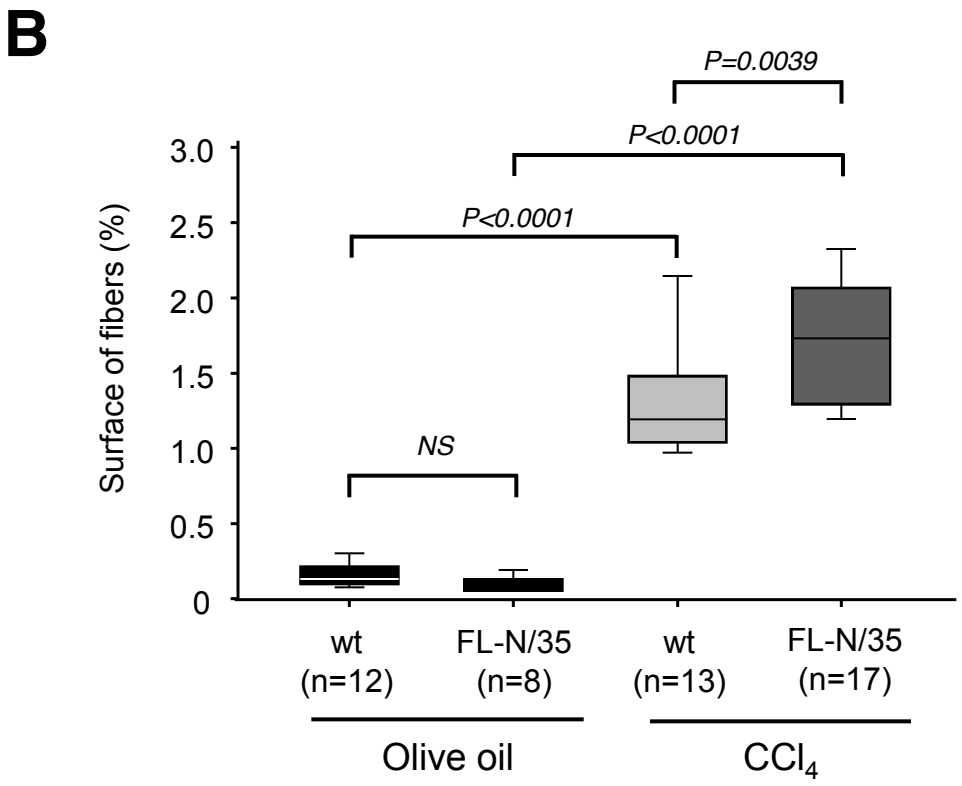
B
P=0.0039
P<0.0001
P<0.0001
NS
Surface of fibers (%)
3.0
2.5
2.0
1.5
1.0
0.5
0
wt
(n=12)
FL-N/35
(n=8)
wt
(n=13)
FL-N/35
(n=17)
Olive oil
CCl4

Figure 2A

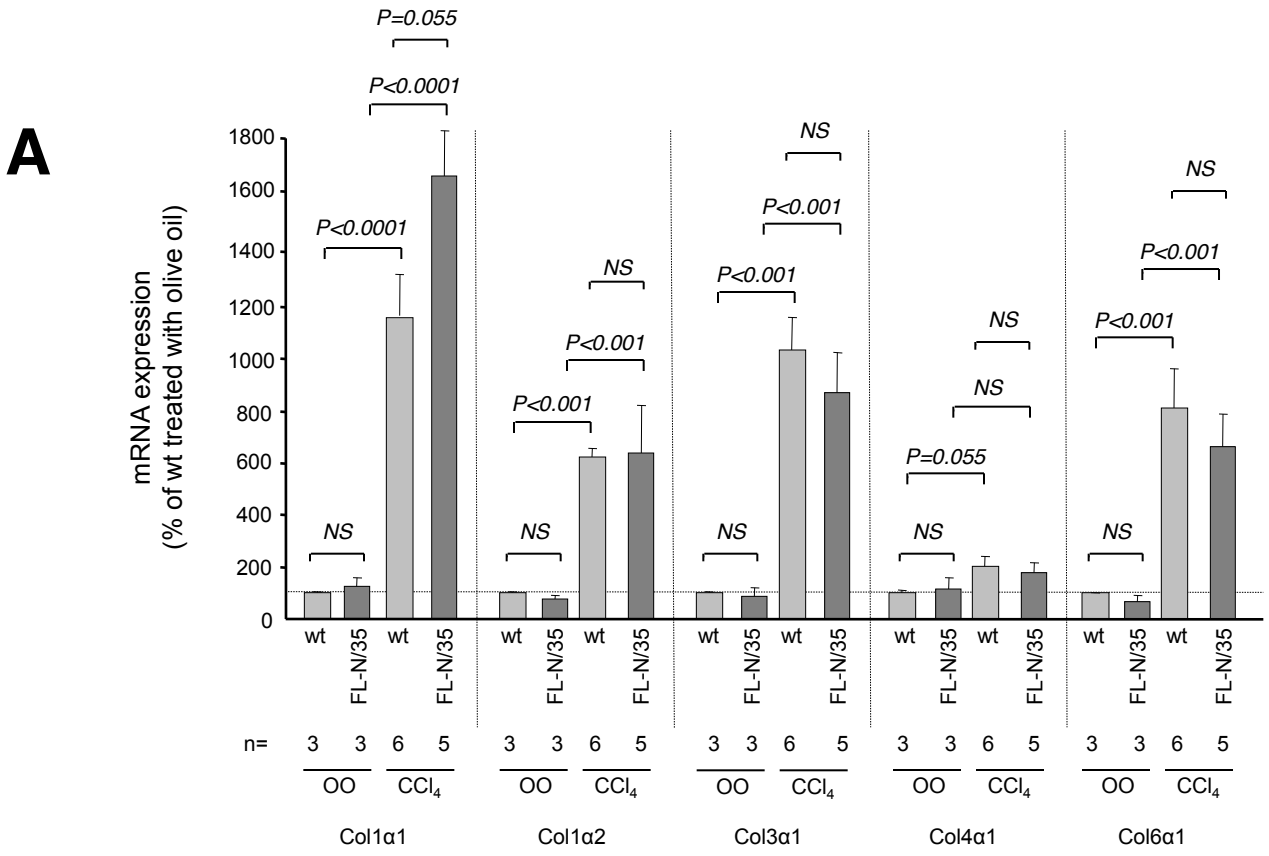
A
mRNA expression
(% of wt treated with olive oil)
1800
1600
1400
1200
1000
800
600
400
200
0
P=0.055
P<0.0001
P<0.0001
NS
P<0.001
NS
P<0.001
NS
P<0.001
NS
P=0.055
NS
P<0.001
NS
NS
NS
NS
NS
wt
FL-N/35
wt
FL-N/35
n=
3 3 6 5
OO
CCl4
Col1α1
Col1α2
Col3α1
Col4α1
Col6α1

Figure 2B

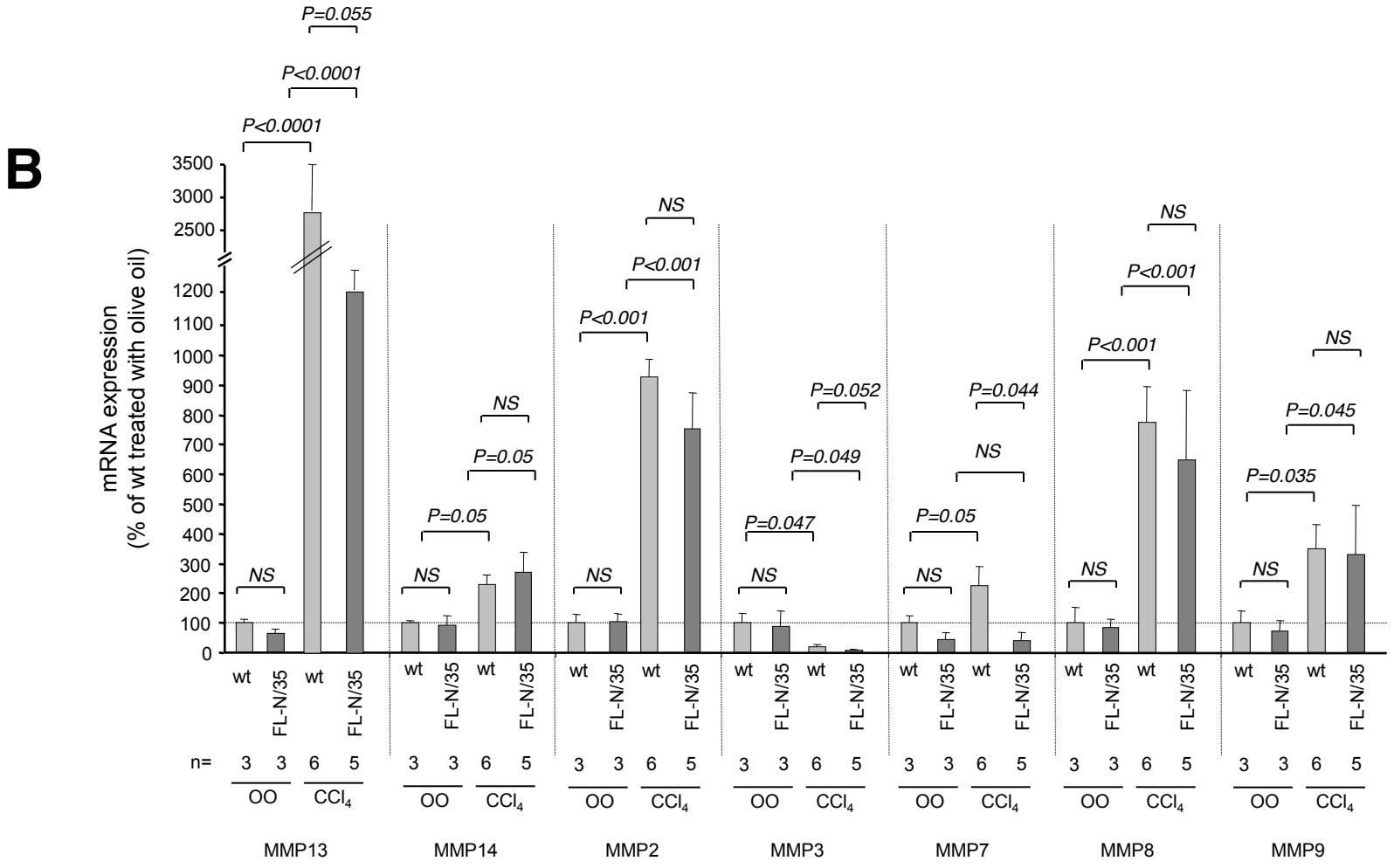
B
mRNA expression
(% of wt treated with olive oil)
3500
3000
2500
1200
1100
1000
900
800
700
600
500
400
300
200
100
0
P=0.055
P<0.0001
P<0.0001
NS
P=0.05
NS
P=0.05
NS
P<0.001
P<0.001
NS
P=0.047
P=0.049
P=0.052
NS
P=0.05
NS
P=0.044
NS
P<0.001
P<0.001
NS
NS
P=0.035
P=0.045
wt
FL-N/35
n=
3 3 6 5
OO
CCl4
MMP13
MMP14
MMP2
MMP3
MMP7
MMP8
MMP9

Figure 2C

C

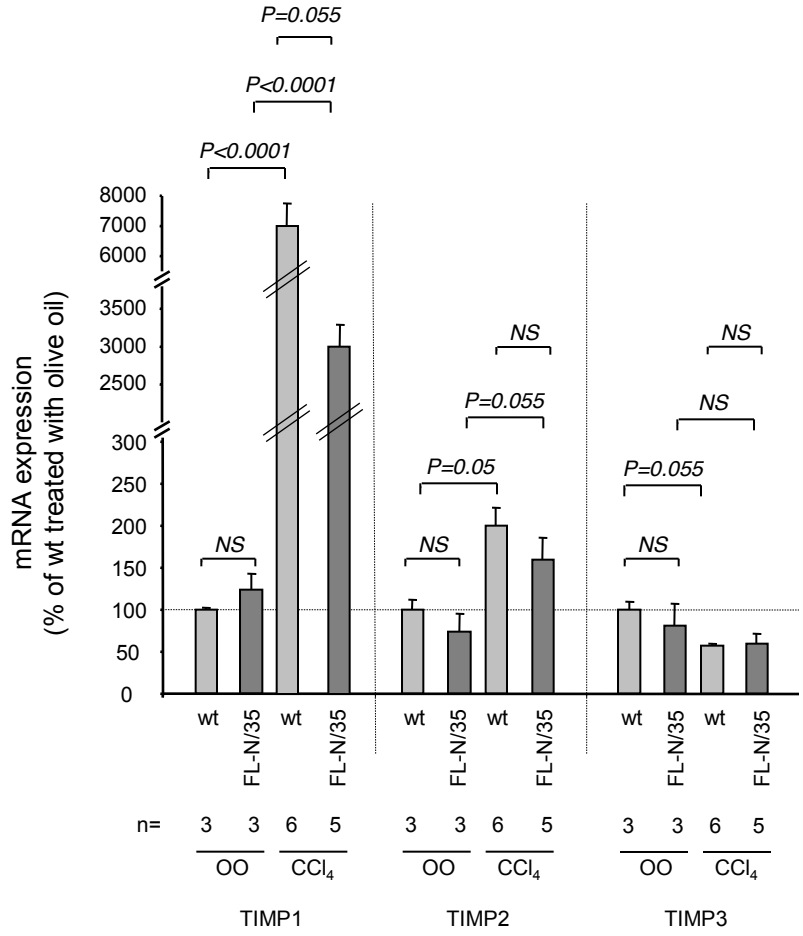
P=0.055
P<0.0001
P<0.0001
mRNA expression
(% of wt treated with olive oil)
8000
7000
6000
3500
3000
2500
300
250
200
150
100
50
0
NS
NS
P=0.055
P=0.05
NS
P=0.055
NS
NS
wt
FL-N/35
wt
FL-N/35
wt
FL-N/35
wt
FL-N/35
wt
FL-N/35
wt
FL-N/35
n=
3 3 6 5
3 3 6 5
3 3 6 5
OO
CCl4
OO
CCl4
OO
CCl4
TIMP1
TIMP2
TIMP3

Figure 3A

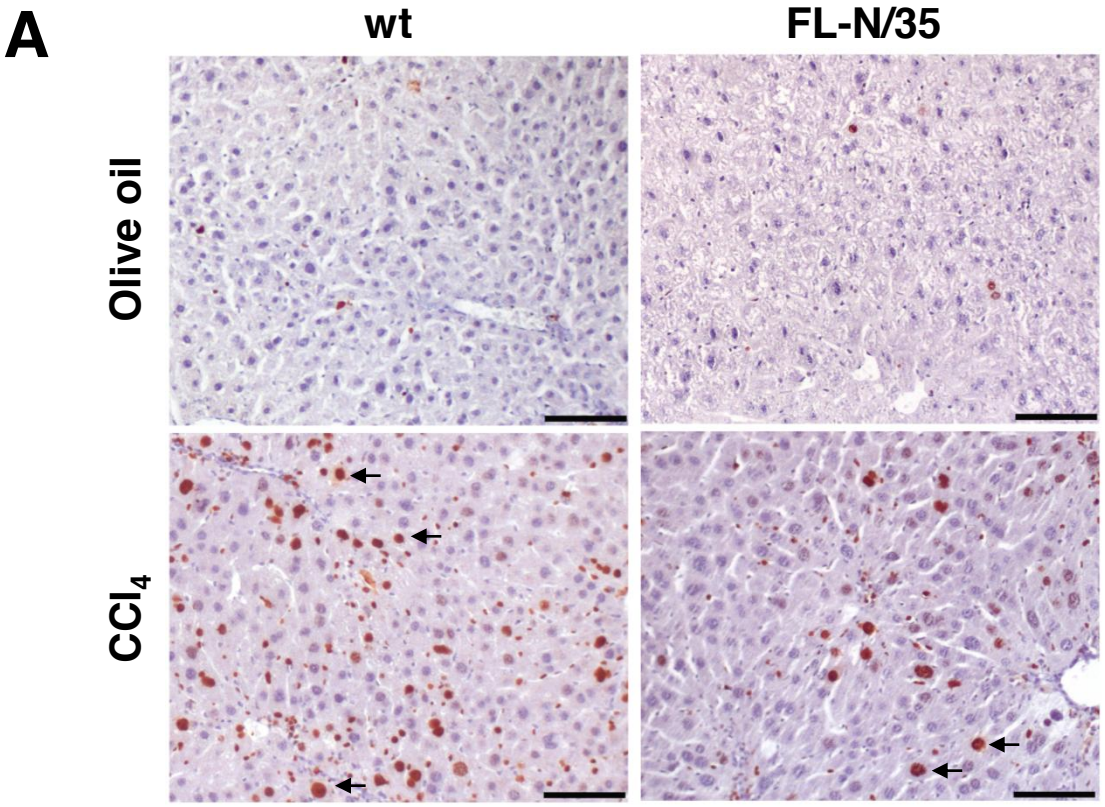

Figure 3B

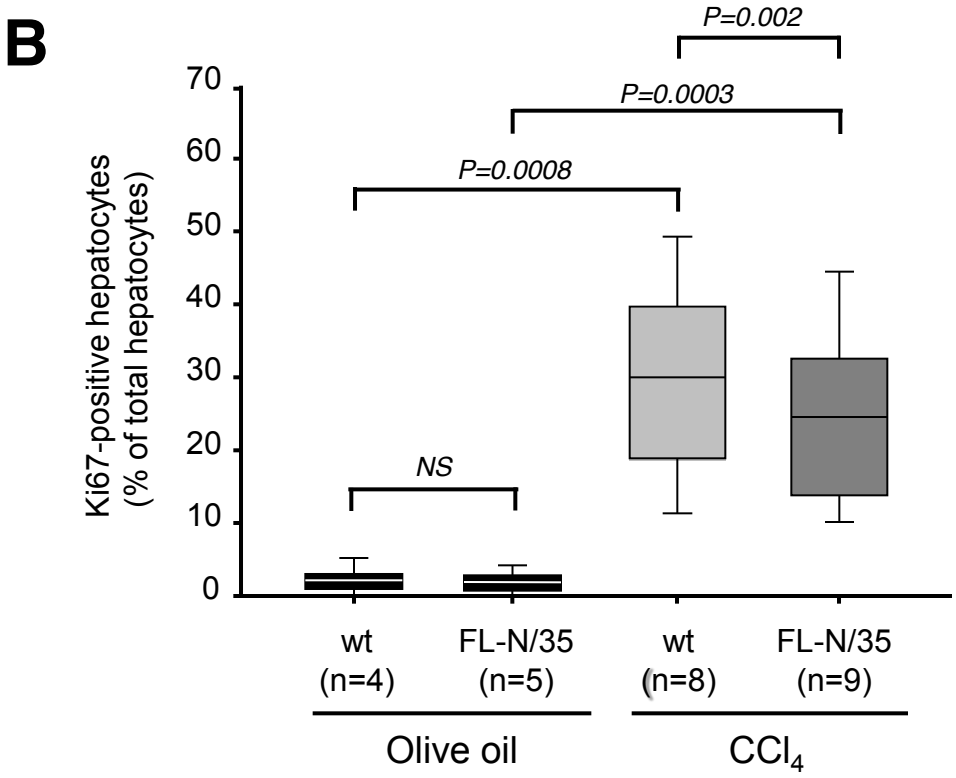
B
P=0.002
P=0.0003
P=0.0008
NS
Ki67-positive hepatocytes
(% of total hepatocytes)
70
60
50
40
30
20
10
0
wt
(n=4)
FL-N/35
(n=5)
wt
(n=8)
FL-N/35
(n=9)
Olive oil
CCl4

Figure 3C

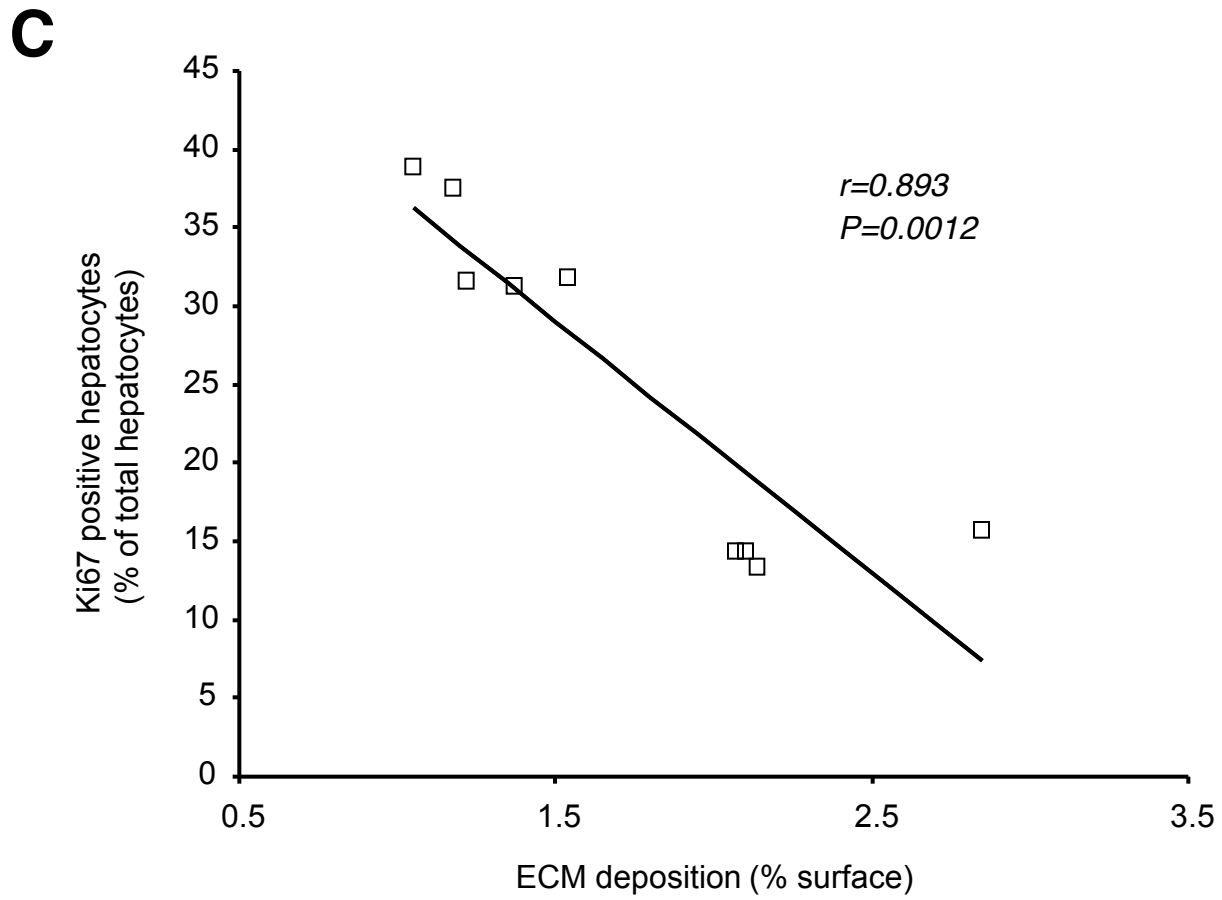
C
45
40
35
30
25
20
15
10
5
0
0.5
1.5
2.5
3.5
Ki67 positive hepatocytes
(% of total hepatocytes)
ECM deposition (% surface)
r=0.893
P=0.0012

Figure 3D

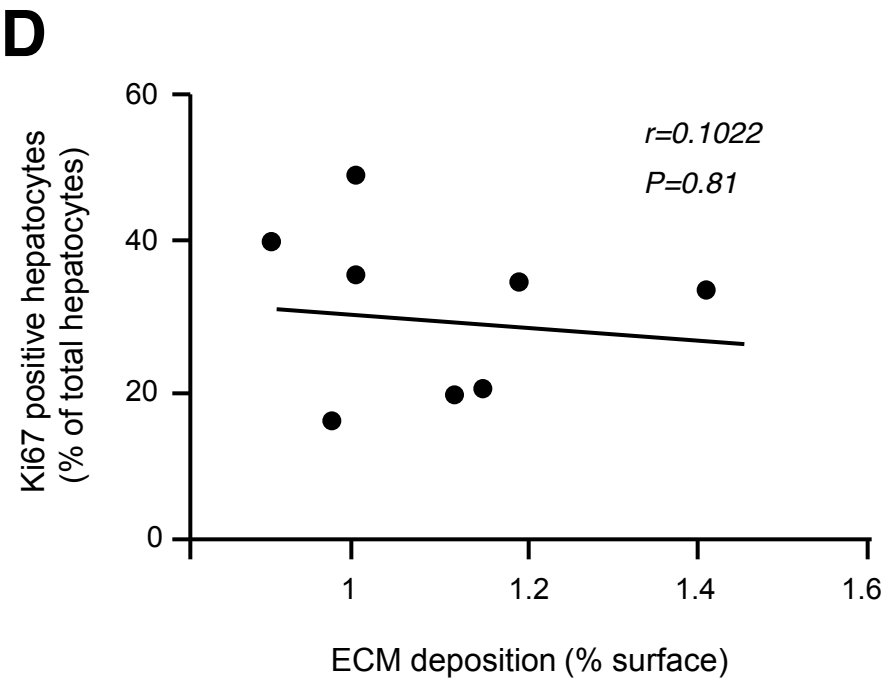
D
60
40
20
0
Ki67 positive hepatocytes
(% of total hepatocytes)
r=0.1022
P=0.81
1
1.2
1.4
1.6
ECM deposition (% surface)

Figure 4A

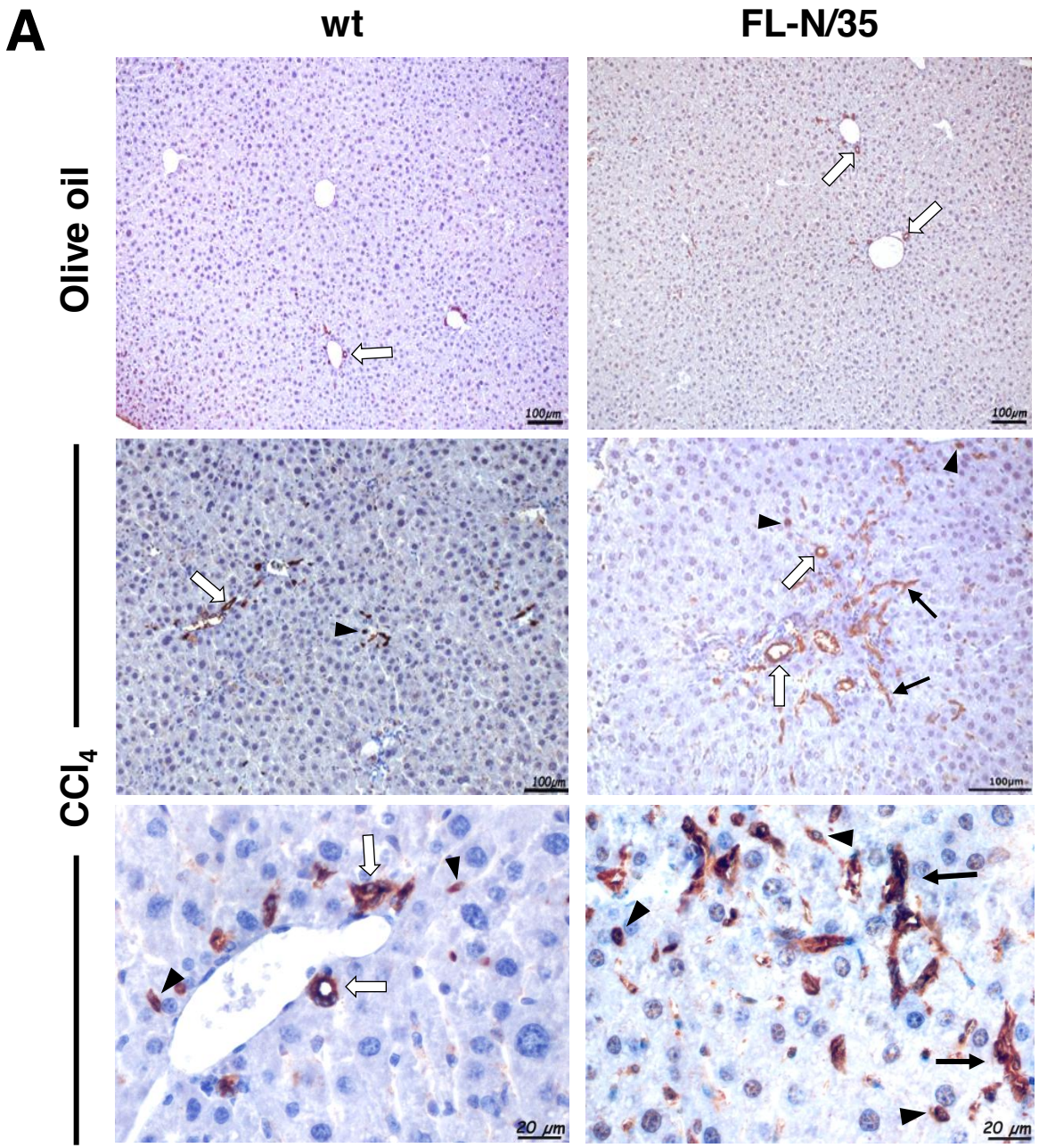

Figure 4B

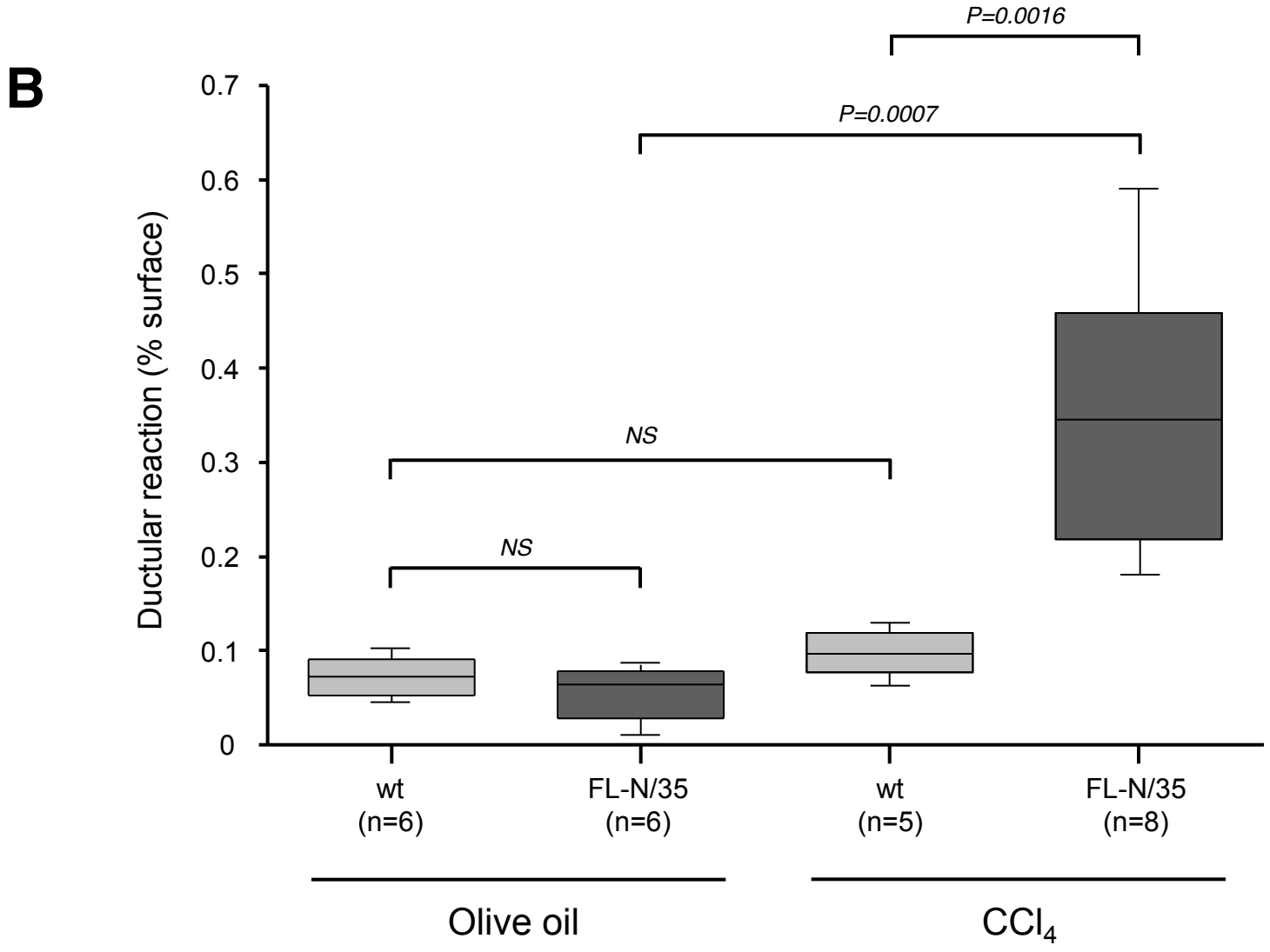
B
P=0.0016
P=0.0007
NS
NS
Ductular reaction (% surface)
0.7
0.6
0.5
0.4
0.3
0.2
0.1
0
wt
(n=6)
FL-N/35
(n=6)
wt
(n=5)
FL-N/35
(n=8)
Olive oil
CCl4

Figure 4C

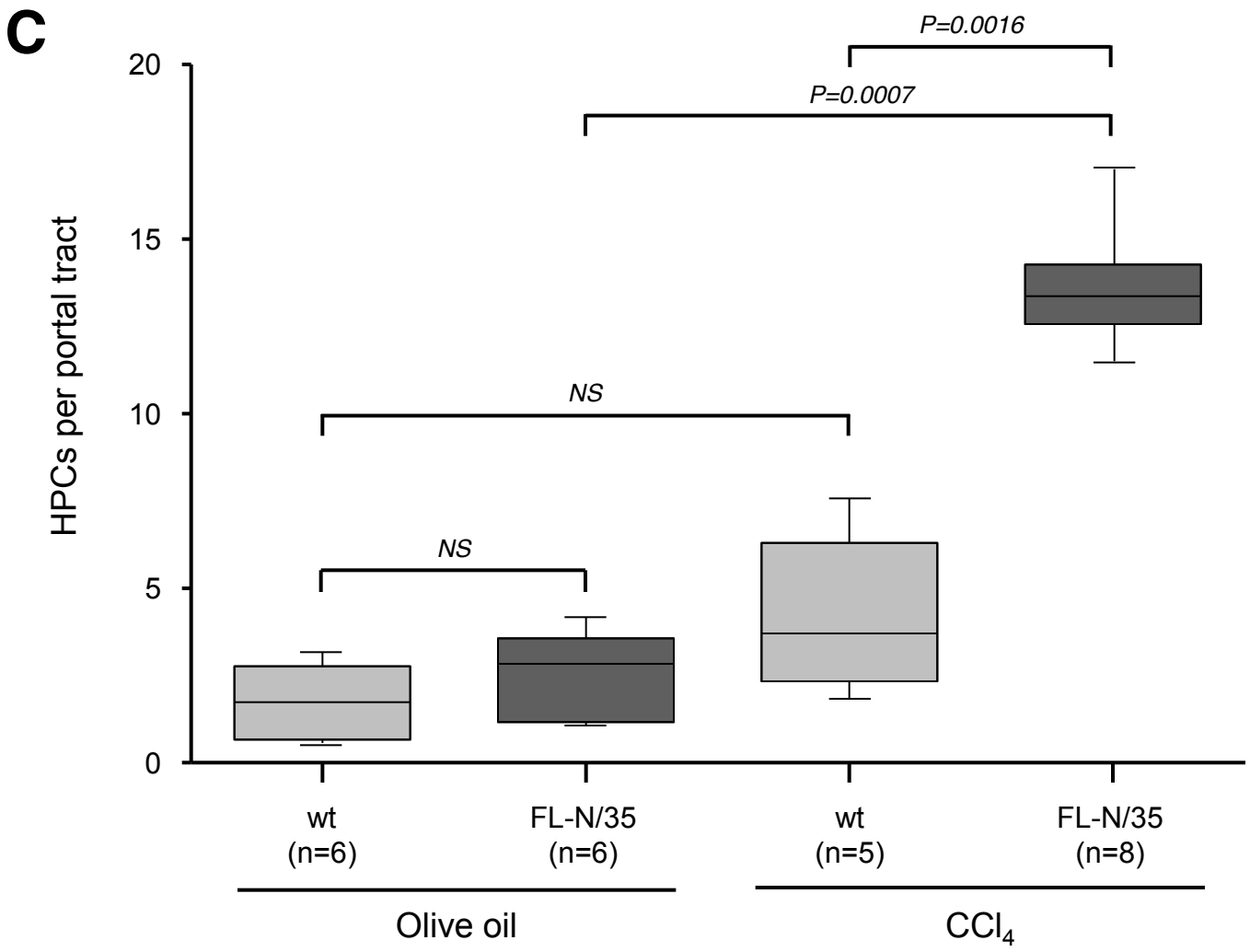
C
P=0.0016
P=0.0007
NS
NS
HPCs per portal tract
20
15
10
5
0
wt
(n=6)
FL-N/35
(n=6)
wt
(n=5)
FL-N/35
(n=8)
Olive oil
CCl4

Figure 4D

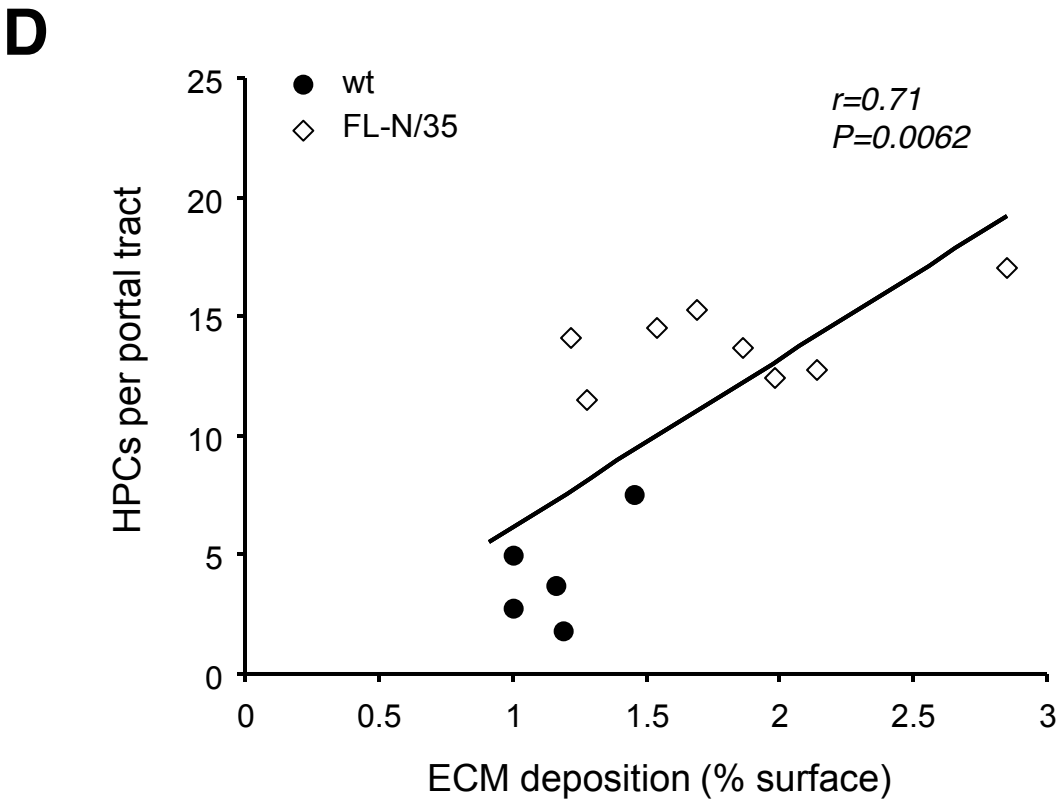
D
wt
FL-N/35
r=0.71
P=0.0062
HPCs per portal tract
ECM deposition (% surface)
0
5
10
15
20
25
0
0.5
1
1.5
2
2.5
3

Figure 4E

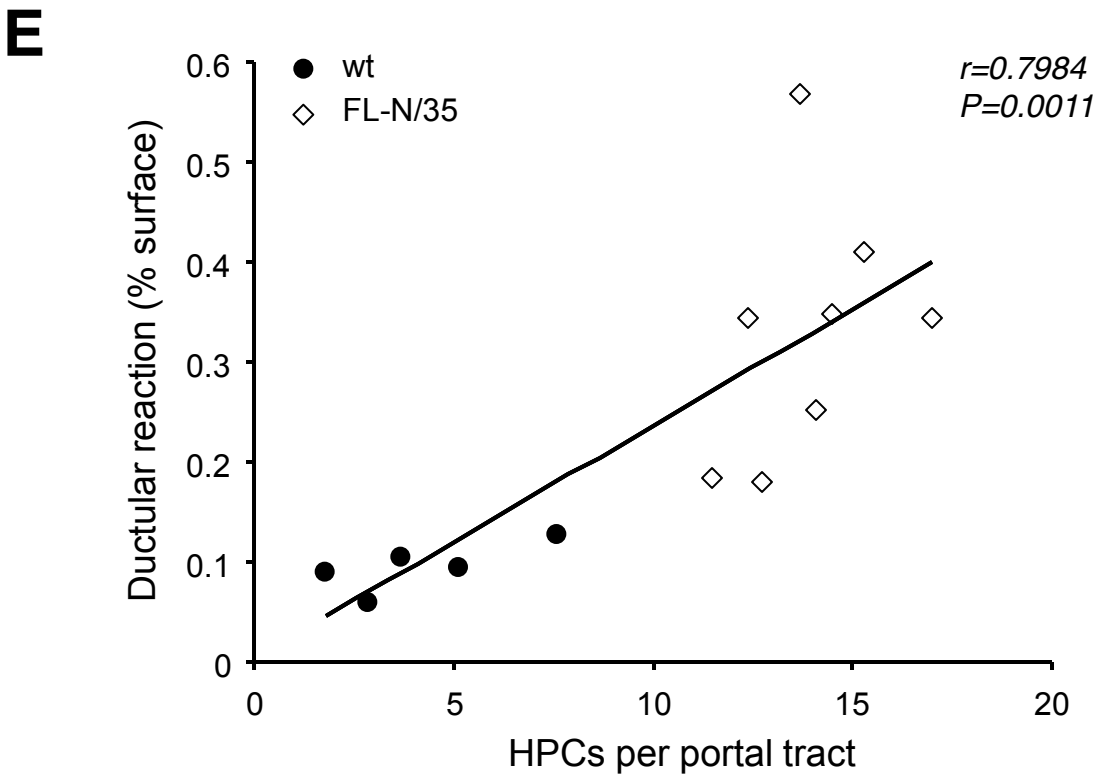
E
wt
FL-N/35
r=0.7984
P=0.0011
Ductular reaction (% surface)
0.6
0.5
0.4
0.3
0.2
0.1
0
0
5
10
15
20
HPCs per portal tract

Figure 5A

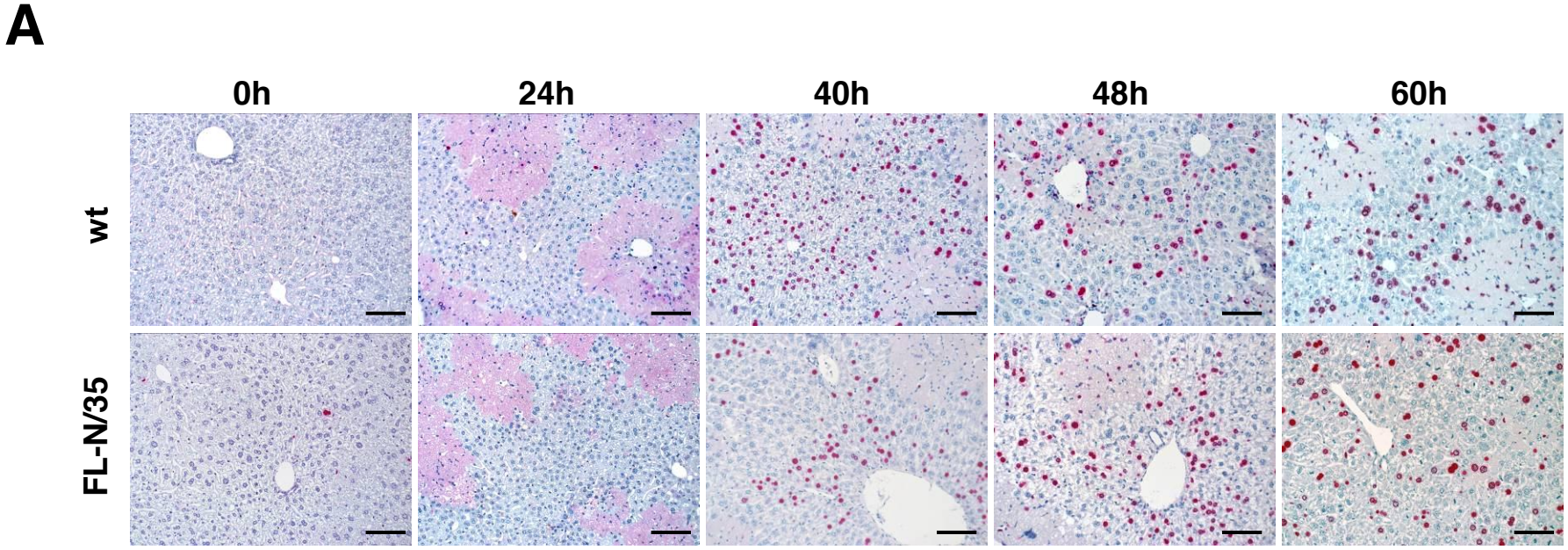

Figure 5B

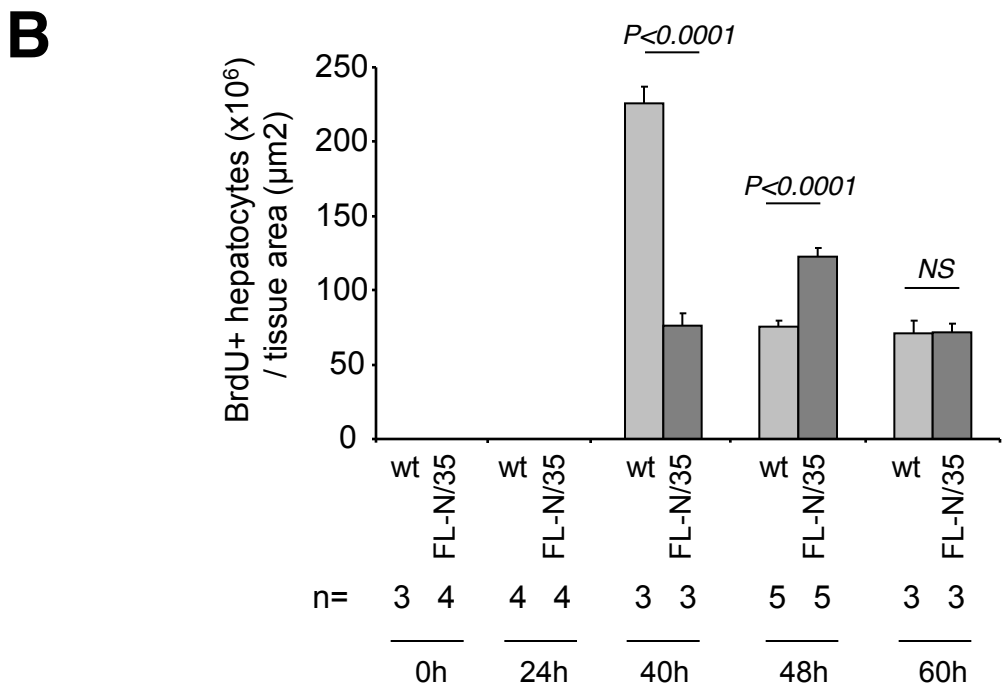
B
P<0.0001
P<0.0001
NS
BrdU+ hepatocytes (x10^6) / tissue area (µm2)
250
200
150
100
50
0
wt
FL-N/35
n=
3 4
4 4
3 3
5 5
3 3
0h
24h
40h
48h
60h

Figure 6A

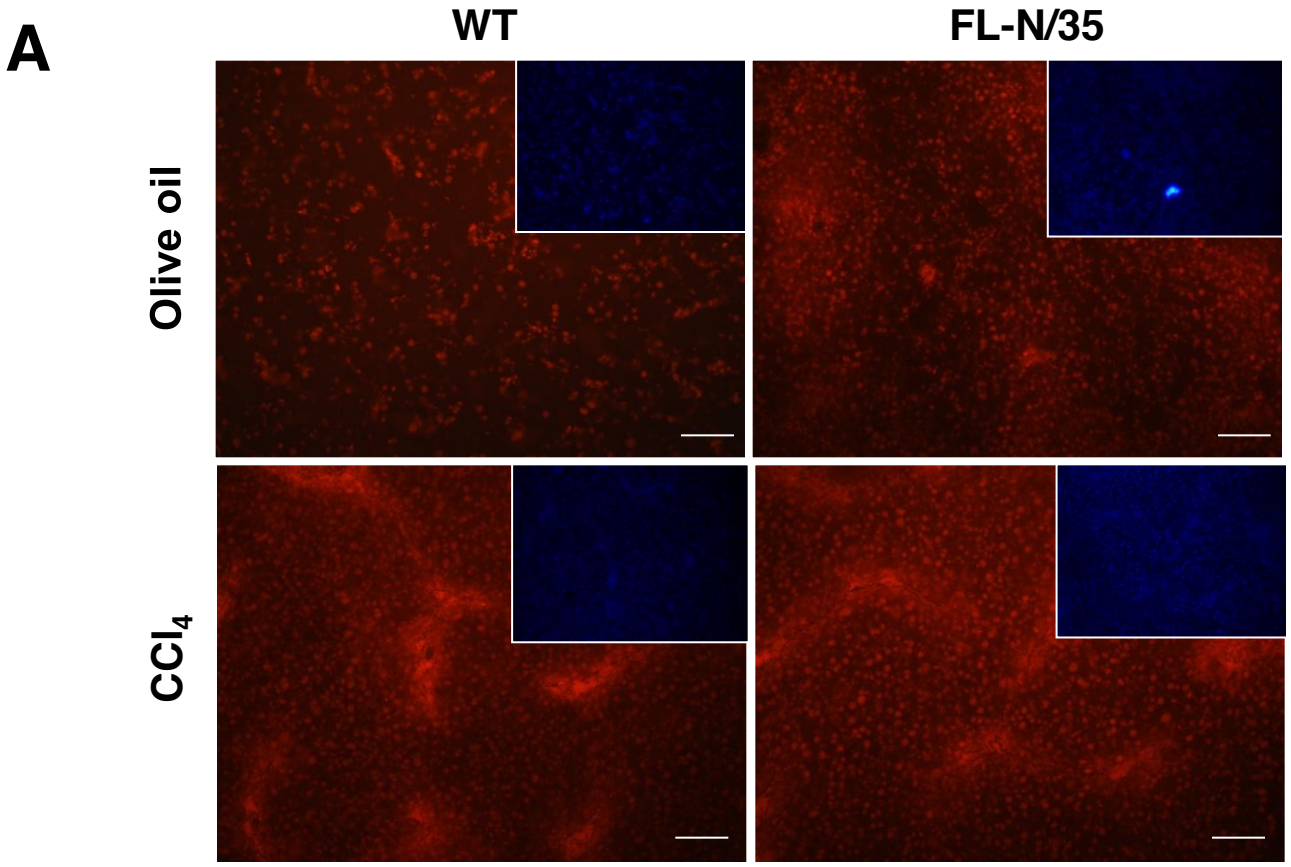

Figure 6B

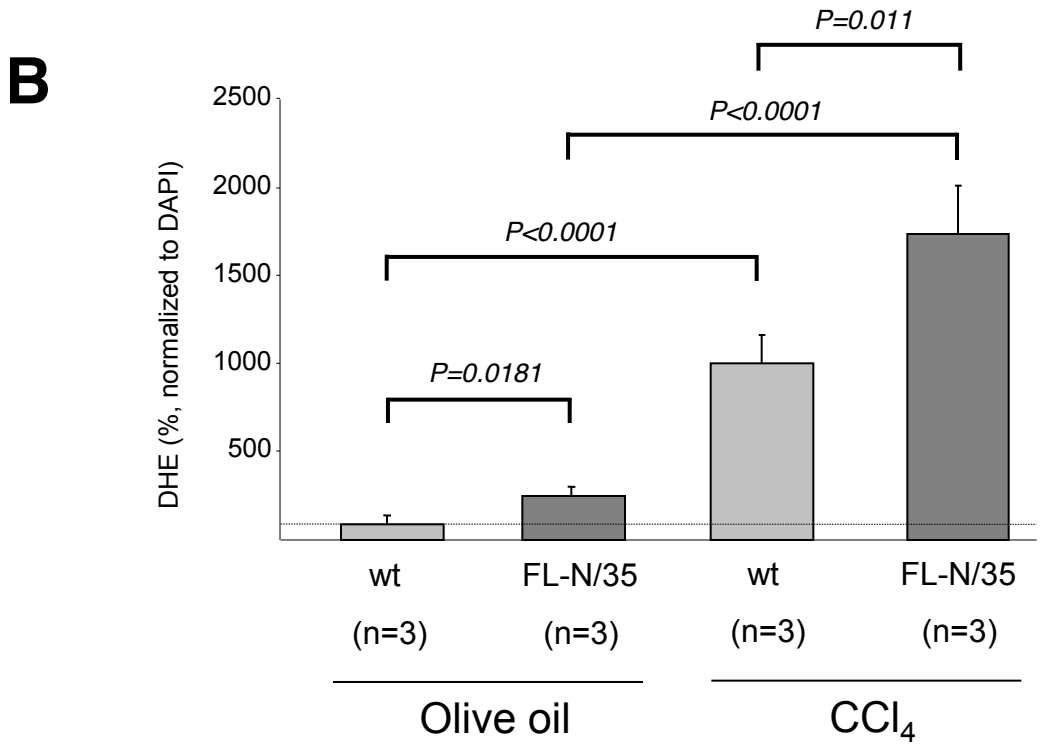
B
P=0.011
P<0.0001
P<0.0001
P=0.0181
2500
2000
1500
1000
500
DHE (%, normalized to DAPI)
wt
FL-N/35
wt
FL-N/35
(n=3)
(n=3)
(n=3)
(n=3)
Olive oil
CCl4

Supplementary Materials and Methods

Click here to download Supplementary material: Supplementary Materials and Methods.doc

Supplementary Figures

Click here to download Supplementary material: Supplementary Figures.ppt